Synthesis and characterization of materials for rechargeable lithium micro-batteries

M. A. Camacho-López,. E. Haro-Poniatowski
Departamento de Física, Laboratorio de Óptica Cuántica, Universidad Autónoma Metropolitana Iztapalapa
Apdo. Postal 55-534, México D. F. 09340, México

L. Escobar-Alarcón
Departamento de Física, Instituto Nacional de Investigaciones Nucleares
Apdo. Postal. 18- 1027, México D. F. 11801, México

C. Julien
Laboratoire des Milieux Désordonnés et Hétérogénes, UMR 7603, Université Pierre et Marie Curie
4 place Jussieu, 72252 Paris cedex 05, France
(Recibido 10 de diciembre de 2002; Aceptado 15 de febrero de 2004)

Pulsed laser deposition was used to grow $LiCoO_2$ and $LiMn_2O_4$ thin films. Crystalline thin films were deposited on silicon at low substrate temperature (300 ^oC) using an oxygen pressure of 50 mTorr for $LiCoO_2$ and 100 mTorr for $LiMn_2O_4$. The structure of these thin film materials was characterized by X-ray diffraction and Raman spectroscopy. The influence of target composition on the stoichiometry of the films was analyzed. Obtained polycrystalline $LiCoO_2$ and $LiMn_2O_4$ thin films were used as cathode materials in lithium micro-batteries. Electrochemical measurements have been performed in both Li//$LiCoO_2$ and Li//$LiMn_2O_4$ thin film cells. These cells were tested by the galvanostatic charge-discharge technique. Specific capacities as high as 195 and 120 mC/cm^2 μm were achieved using $LiCoO_2$ and $LiMn_2O_4$ thin films, respectively.

Keywords: Thin films; Pulsed-laser deposition; Lithium microbatteries

1. Introduction

Among the transition metal oxides, $LiCoO_2$ and $LiMn_2O_4$ are two of the most important materials that have been used as positive electrodes for rechargeable lithium batteries [1]. $LiCoO_2$ and $LiMn_2O_4$ are very attractive materials because lithium-cells based on these materials provide voltages as high as 4 Volt, high specific energy density, and a good reversibility over the lithium insertion-extraction process [2]. It is well known that a suitable crystalline structure of the cathode material is essential for good performance of a micro-battery. It is also well known that $LiCoO_2$ has a layered structure, while $LiMn_2O_4$ has a spinel-framework structure [1, 2].

Thin films of $LiCoO_2$ and $LiMn_2O_4$ have been synthesized by a variety of techniques, including sputtering [3,4] and pulsed laser deposition (PLD) [5-8]. The preparation of Li_xCoO_2 and $Li_xMn_2O_4$ thin films, using the PLD technique, has been reported by Striebel et al. [9]. They obtained crystalline thin films from pure $LiCoO_2$ and $LiMn_2O_4$ powders, on stainless steel substrates. In their experiments they set the substrate temperature at 600 ^oC and a partial oxygen pressure of 100 mTorr during deposition process. Striebel and co-workers studied the electrochemical properties of their PLD films, reporting capacity densities of 62 and 56 μAh/μm cm^2 for $LiCoO_2$ and $LiMn_2O_4$, respectively.

In this work, we present results of the synthesis and characterization of PLD grown $LiCoO_2$ and $LiMn_2O_4$ thin films. Crystalline films have been obtained by the PLD technique on silicon substrates at 300 ^oC. $LiCoO_2$ and $LiMn_2O_4$ targets enriched with Li_2O were used in our experiments. The structural characterization of the films was carried out by X-ray diffraction (XRD) and Raman spectroscopy. The surface morphology of the thin films was analyzed by scanning electron microscopy (SEM). Further in our research, we used the obtained polycrystalline $LiCoO_2$ and $LiMn_2O_4$ thin films as cathode materials to assemble Li//$LiCoO_2$ and Li//$LiMn_2O_4$ cells.

2. Experimental

2.1. Deposition of the thin films

The experimental set-up for growing thin films by pulsed laser deposition has been reported previously [8]. The laser ablation system consist of a vacuum chamber made of stainless steel (evacuated by a turbo-molecular pump) and a pulsed Nd:YAG laser (Lumonics Model HY1200, set to the wavelength of 532 nm and a pulse duration of 10 ns) as the energy source. The target and substrates were placed inside the vacuum chamber as described in reference [8]. The laser beam was focused onto the target with a 15 cm focal length lens at an angle of incidence of 45°. The power density on the target was of the order of 10^8 W/cm^2. During deposition the target was rotated in order to avoid crater formation and to reduce splashing effects. The target-substrate distance was 4 cm and the substrate temperature was 300 °C. The films were deposited on Si(100) substrates which were previously cleaned using distilled water and acetone. The films were grown in an operating partial pressure of oxygen of 50 and 100 mTorr.

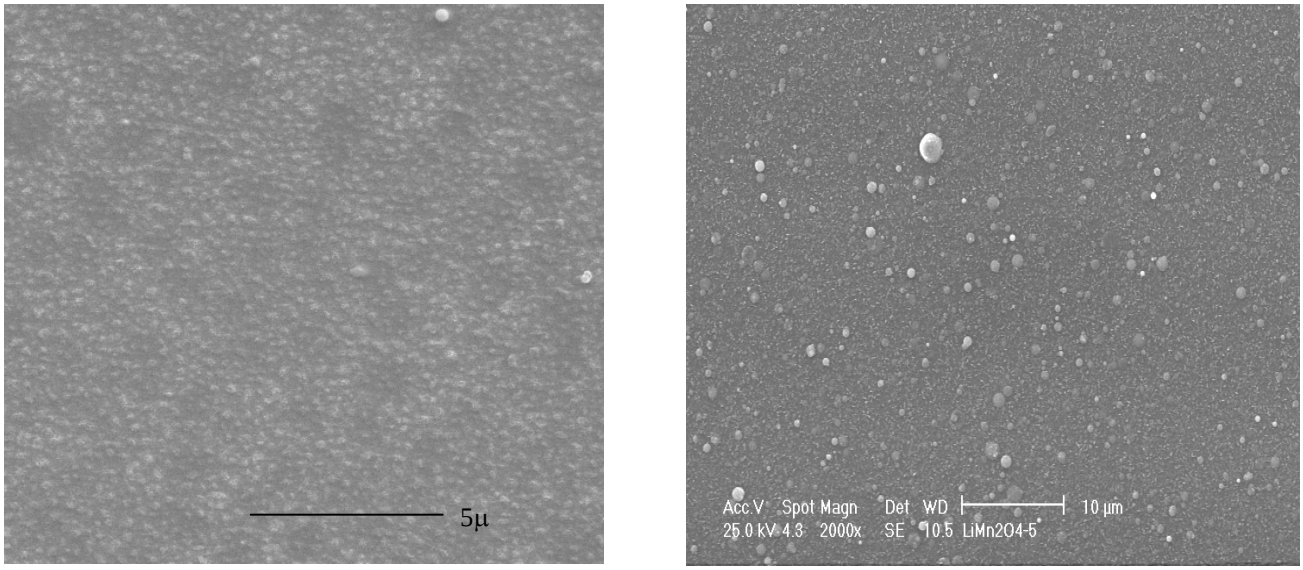

(a) **(b)**

Figure 1. SEM micrographs of the films obtained by PLD technique. a) $LiCoO_2$ + 15 % of Li_2O b) $LiMn_2O_4$ + 15 % of Li_2O.

Different targets were used in this set of experiments; we prepared one target from $LiCoO_2$ powder and the another one from $LiMn_2O_4$ powder. In addition to these targets, we also prepared a set of $LiCoO_2$ and $LiMn_2O_4$ targets enriched with Li_2O having different contents; from 5 to 15 wt%. In all cases the powder was pressed at 5 Ton/cm^2 to form 1.3 cm diameter pellets. These pellets were subsequently thermally treated at 800 °C for 5 hours in air. Table 1 summarizes the growth conditions for the films obtained by the PLD technique.

2.2. Samples characterization

The structure of the $LiCoO_2$ and $LiMn_2O_4$ thin films was characterized by different techniques; X-ray diffraction (XRD) analysis of the films was carried out using a Siemens D-5000 diffractometer with a Cu Kα radiation source (λ= 1.5406 Å). Raman spectra of the thin films were obtained at room temperature with a double monochromator Spex model 1403 and an Argon-ion laser (Laser ionics), the integration time was 1 s for each incremental step of 1 cm^{-1}. The surface morphology of the films was observed by scanning electron microscopy (SEM) with a Phillips XL-30 microscope.

Electrochemical measurements were performed on Li//$LiCoO_2$ and Li//$LiMn_2O_4$ cells manufactured with a lithium metal foil as anode over the obtained $LiCoO_2$ and $LiMn_2O_4$ thin films as cathodes; having a 1.5 cm^2 active area in a Teflon home-made cell hardware. The silicon substrate was connected with a silver wire using silver paint and covered by insulating epoxy leaving only the film as active area. The electrolyte consisted of 1 M $LiClO_4$ dissolved in propylene carbonate.

3. Results and discussion

3.1. Scanning Electron Microscopy

Figure 1 shows the SEM micrographs corresponding to the $LiCoO_2$ and $LiMn_2O_4$ thin films obtained at 300 °C; these thin films were grown from targets enriched with 15 % of Li_2O. In both micrographs, one can see the formation of discrete particles at the surface of the layer, which gives the surface its roughness. In both cases, the films exhibit a surface roughness with small grains. The layers that constitute the materials deposited have a good density.

Table 1. Growth conditions to obtain $LiCoO_2$ and $LiMn_2O_4$ thin films by Pulsed Laser Deposition.

Sample	**Substrate temperature** (°C)	**Oxygen partial pressure** (mTorr)	**Li_2O Content** (wt %)
0LICO	300	50	0
5LICO	300	50	5
10LICO	300	50	10
15LICO	300	50	15
0LIMN	300	100	0
5LIMN	300	100	5
10LIMN	300	100	10
15LIMN	300	100	15

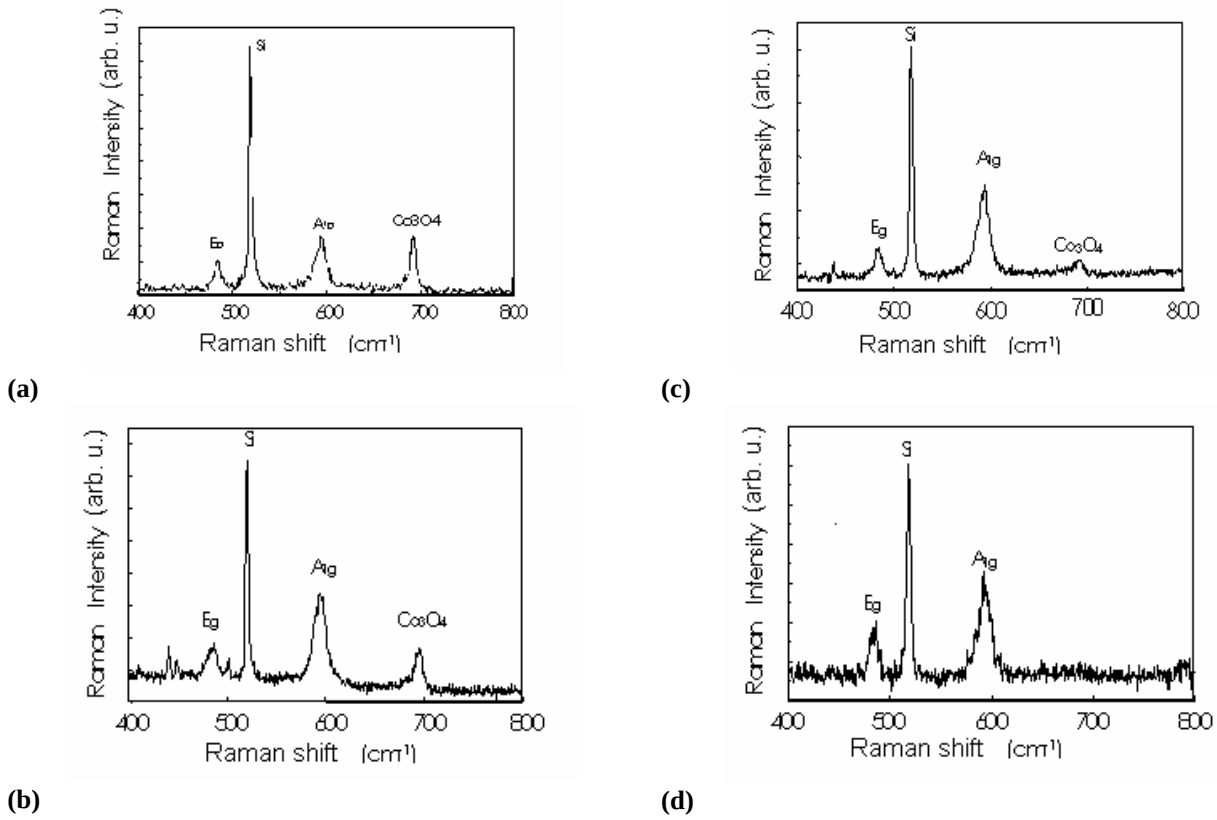

Figure 2. Raman spectra of $LiCoO_2$ thin films deposited from targets with different content of Li_2O. a) 0 %, b) 5 %, c) 10 %, and d) 15 %.

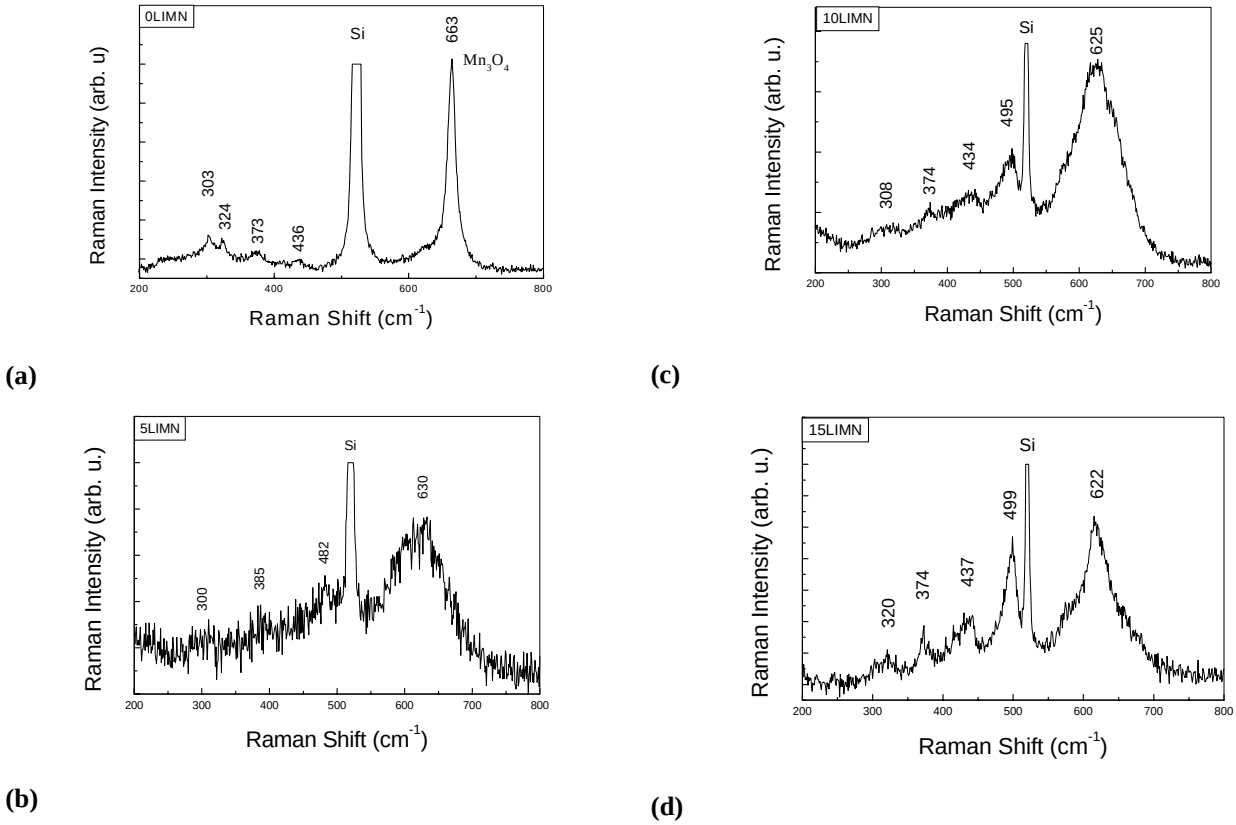

Figure 3. Raman spectra of $LiMn_2O_4$ thin films deposited from targets with different content of Li_2O. a) 0 %, b) 5 %, c) 10 %), and d) 15 %.

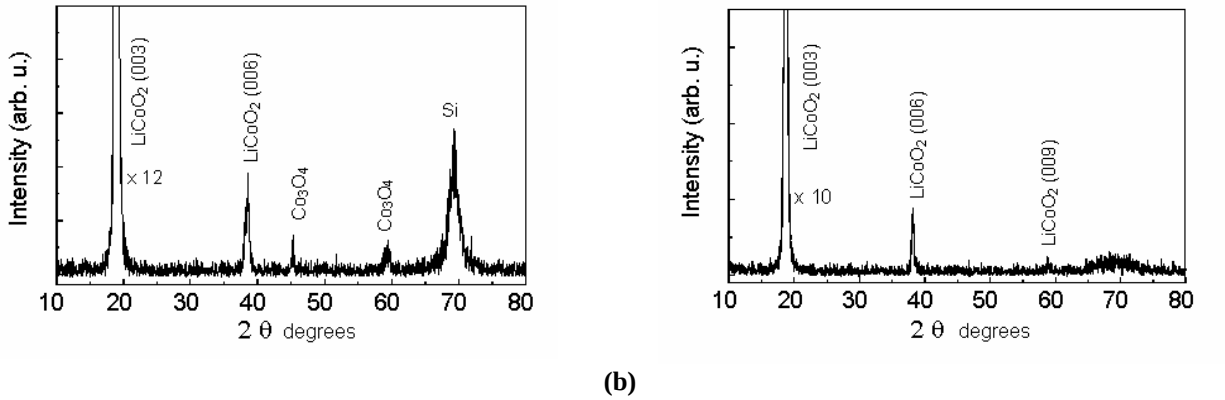

Figure 4. X- ray diffraction patterns for the films grown from a) $LiCoO_2$ without Li_2O and b) $LiCoO_2$ + 15 % of Li_2O.

This is directly related to the average grain size, which is approximately 100 nm. One of the main features of the films obtained by the PLD technique is their high density compared with that found in films grown by conventional techniques. C. Chen et al. have deposited $LiCoO_2$ films by using electrostatic spray deposition technique [10]. Surface morphology of their films was constituted by large particles with sizes between 4 and 20 μm giving low-density films.

3.2. Raman spectroscopy

a. $LiCoO_2$

Raman spectra of thin films deposited from targets with different content of Li_2O are showed in figure 2 (a-d). A strong peak centered at 521 cm^{-1} is present in all the spectra; it corresponds to the silicon substrate. The peaks centered at 484 and 595 cm^{-1} correspond to the two allowed Raman modes of layered $LiCoO_2$ crystal [10]. This result is in good agreement with the factor group analysis of the R3m symmetry. For the $LiMO_2$ (M=Co,Cr,Ni) family a general rule is that the two active Raman modes are located in the range between 400 and 650 cm^{-1} [10]. The peak center at 693 cm^{-1} is assigned to a mode vibration of Co_3O_4 species; the presence of this species is due to the lithium loss during the deposition process. This peak is not present in Raman spectrum 2d, which corresponds to the film grown from a target with 15 % of Li_2O. This indicates that Co_3O_4 and layered $LiCoO_2$ phases are formed when Li_2O content in the target is between 0% and 10%. The optimum concentration of Li_2O to compensate the lithium loss lies between 10% and 15 %. With a Li_2O concentration of 15% only the layered $LiCoO_2$ phase is obtained.

b. $LiMn_2O_4$

Figure 3(a-d) shows the Raman spectra of thin films deposited from targets with different Li_2O content. These Raman spectra correspond to the thin films grown on silicon kept at 300 °C in an oxygen partial pressure of 100 mTorr. In that case, the spectra show a peak centered at 521 cm^{-1} which, as pointed out above, corresponds to the silicon substrate. The presence of a peak centered at 663 cm^{-1} in the spectrum of the sample grown with a pure $LiMn_2O_4$ target (3a) indicates the formation of Mn_3O_4 during the deposition process. This peak is characteristic of all the spinel structures like Fe_3O_4. As it occurs in the case of $LiCoO_2$ the formation of this undesired oxide is due to the lithium loss, and we can eliminate that effect using lithium-rich targets. It is worth noting that using an enriched target with 5 wt%, the peak assigned to Mn_3O_4 disappears and the Raman spectrum is constituted only by features related to $LiMn_2O_4$. The same result is obtained by using enriched targets with high Li_2O content (10 and 15 %wt). From spectra 3b, 3c and 3d we can identify a systematic shift towards low frequencies of the broad-peak (centered around 625 cm^{-1}), and a reduction of its full width at half maximum (FHWM), indicating that the degree of crystallinity improves when lithium-rich targets are used. In that case, a Li_2O concentration of 15% seems to be adequate to grow crystalline thin films with the correct stoichiometry. Factor group analysis predicts five Raman-active modes (A_{1g}, + E_g + $3F_{2g}$) for the Fd3m symmetry. Raman spectrum 3d presents five broad band peaks located at 320, 374, 437, 499, 622 cm^{-1} and the last one has a shoulder at 580 cm^{-1}. The main band (at 622 cm^{-1}) has A_{1g} symmetry and corresponds to the symmetric Mn-O stretching vibration of MnO_6 groups. The bands at 374 and 437 cm^{-1} can be assigned to the Li-O vibrations of LiO_4 groups. The band at 320 cm^{-1} might correspond to the bending vibration of MnO_6 groups [11]. These Raman results clearly indicate that films obtained from the target with a Li_2O concentration of 15% have a spinel-type structure.

3.3. X-ray diffraction

a. $LiCoO_2$

In order to confirm the Raman spectroscopy results presented above, we carried out x-ray diffraction (XRD) measurements. Figure 4 shows the x-ray diffractogram of the 0LICO and 15LICO thin films. Two small peaks attributed to Co_3O_4 are present in the diffractogram 4a; the

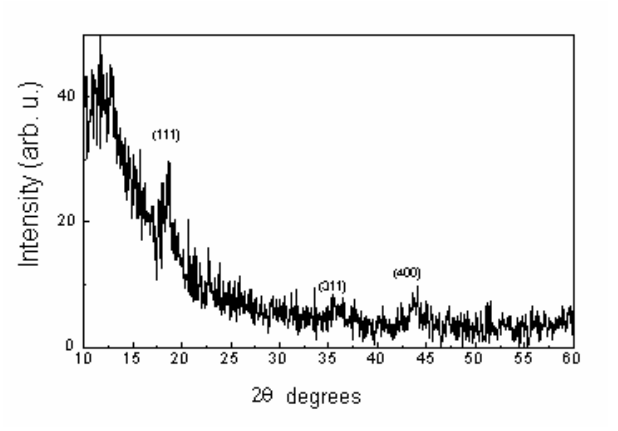

(a)

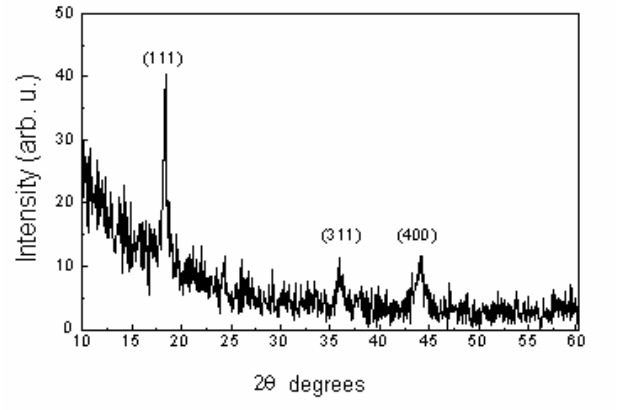

(b)

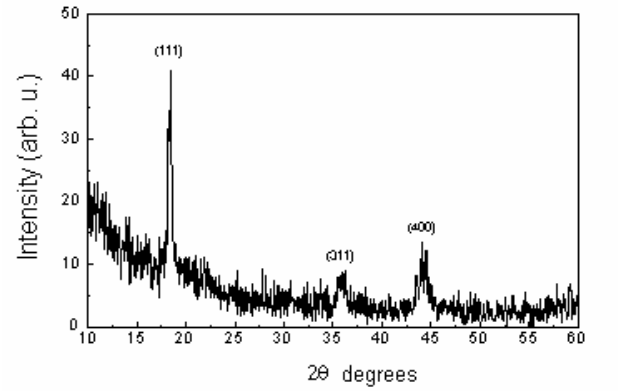

(c)

Figure 5. X- ray diffraction patterns for the films grown from a) $LiMn_2O_4$ + 5 % of Li_2O, b) $LiMn_2O_4$ + 10 % of Li_2O and c) $LiMn_2O_4$ + 15 % of Li_2O.

diffractogram also shows two peaks attributed to $LiCoO_2$. The peak around 70 degrees is associated to the silicon substrate. The diffractogram of the 15LICO film is shown in figure 4b, notice the absence of peaks attributed to Co_3O_4. Notice also the presence of three sharp and intense peaks corresponding unambiguously to the (003), (006) and (009) reflections of highly oriented $LiCoO_2$ film. The lower intensity of the silicon peak is probably due to a major thickness of this film.

b. $LiMn_2O_4$

Figure 5 shows the diffractograms of $LiMn_2O_4$ films as a function of target composition. From figure 5a one can see that 5LIMN film is poorly crystallized and there is not evidence of the Mn_3O_4 phase, in total accordance with the Raman results. However, as the amount of Li_2O increases in the target, the corresponding XRD pattern clearly indicates improved crystallization. Diffractogram 5c corresponds to the 15LIMN film and shows peaks at 2θ= 16, 36 and 47 degrees which are attributed to the (111), (311) and (400) Bragg planes, respectively. These x-ray diffraction results conclusively confirm the results we previously obtained by Raman spectroscopy.

3.3. Electrochemical studies

$LiCoO_2$ and $LiMn_2O_4$ thin films with the best crystalline structure (15LICO and 15LIMN) were employed as cathode materials in electrochemical studies. Li//$LiCoO_2$ and Li//$LiMn_2O_4$ cells were tested using 1 M $LiClO_4$ dissolved in propylene carbonate as electrolyte. Figure 6 shows the typical charge-discharge curves of cells manufactured using (a) 15LICO and (b) 15LIMN films as positive electrodes. From these charge-discharge curves one can observe that in the voltage range 2.0 - 4.2 V and 3.2- 4.2 V, the specific capacity delivered by $LiCoO_2$ and $LiMn_2O_4$ active films was of 195 mC/cm^2 μm and 120 mC/cm^2 μm, respectively. These specific capacities are superior to those reported by Striebel and co-workers [9].

4. Conclusions

Layered $LiCoO_2$ and spinel $LiMn_2O_4$ thin films were obtained by pulsed laser deposition. Structural properties of these films were investigated as a function of the target composition. Raman studies of the thin films grown from pure $LiCoO_2$ and $LiMn_2O_4$ targets allowed us to identify that the Co_3O_4 and Mn_3O_4 impurity phases are formed in the films, respectively. When Li_2O enriched targets with a content of 15 wt% were used, the films obtained were pure $LiCoO_2$ and $LiMn_2O_4$ as shown by Raman spectroscopy and confirmed later by X-ray diffraction.

Both, $LiCoO_2$ and $LiMn_2O_4$ PLD thin films were implemented as positive electrodes in Li//$LiCoO_2$ and Li//$LiMn_2O_4$ micro-batteries, respectively. The specific capacity delivered by $LiCoO_2$ and $LiMn_2O_4$ active films, in the voltage range from 2.0 to 4.2 V and from 3.2 to 4.2 V, was 195 mC/cm^2 μm and 120 mC/cm^2 μm, respectively. Our results show clearly indication that the pulsed laser deposition process can be used to grow thin film materials with very promising features for its integration in lithium micro-batteries technology.

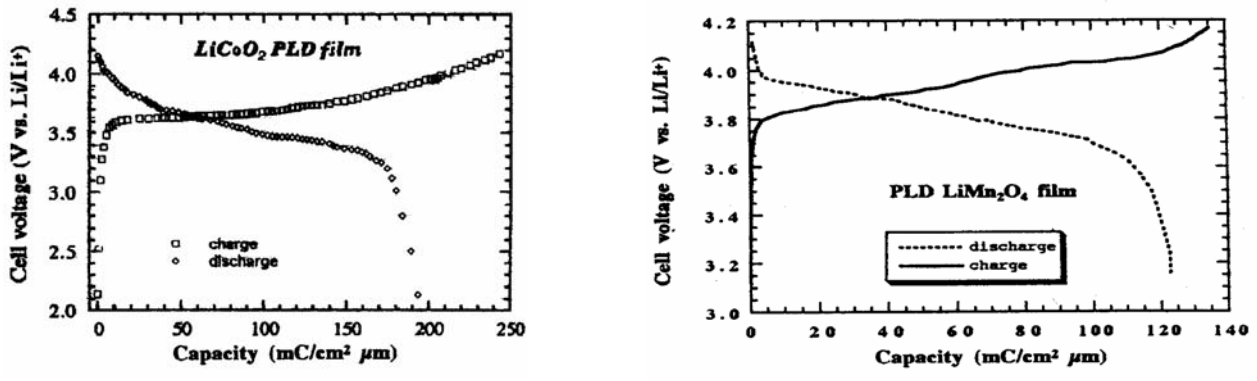

(a) **(b)**

Figure 6. Charge-discharge curves of a) Li//$LiCoO_2$ and b) Li// $LiMn_2O_4$ cells using $LiCoO_2$ and $LiMn_2O_4$ PLD films respectively.

Acknowledgements

M. A. Camacho-López acknowledges support from CONACyT (México) for this research project.

References

[1] C. Julien and G. A. Nazri, Solid-State Batteries : Materials Design and Optimization, Kluwer (1994).
[2] T. Ohzuku, Lithium Batteries, New Materials, Developments and Perspectives, Elsevier, Amsterdam (1993)
[3] E. J. Plichta, W. K. Behl J. Electrochem. Soc. **140**, 46 (1993).
[4] K. H. Hwang, S. H. Lee, S. K. Joo, J. Electrochem. Soc. **141**, 3296 (1994).
[5] M. Antaya, K. Cearns, J. S. PrestonJ.N.Reimers, J.R. Dahn , J. Appl. Phys. **76**, 2799 (1994).
[6] M. Morcrette, P. Barboux, J. Pierriere, T. Brousse, Solid State Ionics. **112**, 249 (1998).
[7] C. Julien, M. A. Camacho-López, L. Escobar-Alarcón E. Haro-Poniatowski, Materials Chemistry and physics. **68**, 210 (2001).
[8] C. Julien E. Haro-Poniatowski M. A. Camacho-López L. Escobar-Alarcón, J. Jiménez-Jarquín, Materials Science and Engineering B. **72**, 36 (2000).
[9] K.A. Striebel, C. Z. Deng, S. J. Wen, E. J. Cairns, J. Electrochem. Soc. **143**, 1821 (1996).
[10] C. Chen, E. M. Kelder, P. J.J.M van der Put, J. Schoonman, J. Mater. Chem. **6**, 765 (1996).
[11] C. Julien, M. Massot, C. Perez-Vicente, E. Haro-Poniatowski, G. A. Nazri, A. Rougier, Mat. Res. Soc. Symp. Proc. **496**, 415 (1998).